



# Latitudinal temperature gradient during the Cretaceous Upper Campanian–Middle Maastrichtian: $\delta^{18}\text{O}$ record of continental vertebrates

Romain Amiot<sup>a</sup>, Christophe Lécuyer<sup>a,\*</sup>, Eric Buffetaut<sup>b</sup>, Frédéric Fluteau<sup>c</sup>,  
Serge Legendre<sup>a</sup>, François Martineau<sup>a</sup>

<sup>a</sup>Laboratoire Paléoenvironnements and Paléobiosphère, CNRS UMR 5125, Université Claude Bernard Lyon I,  
27–43 bld du 11 Novembre 1918, 69622 Villeurbanne, France

<sup>b</sup>CNRS, 16 cours du Liébat, 75013 Paris, France

<sup>c</sup>Laboratoire de Paléomagnétisme, CNRS UMR 7577, Institut de Physique du Globe de Paris, 4 place Jussieu,  
75252 Paris cedex 05, France

Received 14 May 2004; received in revised form 9 July 2004; accepted 13 July 2004

Editor: V. Courtillot

## Abstract

Latitudinal variations in model biogenic apatite  $\delta^{18}\text{O}$  values were calculated using fractionation equations of vertebrates and weighted rainfall  $\delta^{18}\text{O}$  values along with mean annual air temperatures provided by IAEA–WMO meteorological stations. The reference equation obtained was used to compute a continental temperature gradient for the Late Campanian–Middle Maastrichtian interval by using published and new  $\delta^{18}\text{O}$  values of phosphate from vertebrates. Samples are mainly tooth enamel from crocodylians and dinosaurs that lived at paleolatitudes ranging from  $83_{-9}^{+4}\text{N}$  (Alaska) to  $32\pm 3\text{S}$  (Madagascar). The temperature gradient was less steep ( $0.4\pm 0.1\text{ }^{\circ}\text{C}/^{\circ}\text{latitude}$ ) than the present-day one ( $0.6\text{ }^{\circ}\text{C}/^{\circ}\text{latitude}$ ) with temperatures that decreased from about  $30\text{ }^{\circ}\text{C}$  near the equator to about  $-5\text{ }^{\circ}\text{C}$  at the poles. Above  $30^{\circ}$  of paleolatitude, air temperatures were higher than at present. The validity of these results is discussed by comparison with climatic criteria inferred from paleontological, paleobotanical and sedimentological data. The latitudinal distribution of oxygen isotope compositions of continental vertebrates is potentially a powerful tool for quantifying Mesozoic terrestrial climates.

© 2004 Elsevier B.V. All rights reserved.

*Keywords:* Late Cretaceous; oxygen isotopes; vertebrates; apatite; continental climate

## 1. Introduction

For decades, the Cretaceous has been considered as the warmest period of the Phanerozoic, with

\* Corresponding author. Also at the Institut Universitaire de France. Fax: +33 4 7243 1688.

*E-mail address:* [clecuyer@univ-lyon1.fr](mailto:clecuyer@univ-lyon1.fr) (C. Lécuyer).

relatively equable climates [1–3]. Although recent studies have suggested the existence of cool periods during the Cretaceous [4–7], some climatic stages are recognized as having been especially warm, such as the Cenomanian–Turonian interval, supposedly as a result of high levels of atmospheric CO<sub>2</sub> (up to four times the Present Atmospheric Level; e.g., [8]), high sea-levels [9] and changes in oceanic circulation patterns in relation to plate motions (e.g., [10]). Most quantitative determinations of seawater paleotemperatures were derived from <sup>18</sup>O/<sup>16</sup>O ratios of oceanic Cretaceous sediments sampled during the Ocean Drilling Project (ODP) campaigns. These data partly contributed to estimate thermal variations as a function of latitude. Knowledge of latitudinal thermal gradients is critical to define climatic modes because they reflect the presence or absence of polar ice caps and the dynamics of heat transfer from low to high latitudes. The distribution of temperatures at the Earth's surface is also fundamental to relate biodiversity to climate and more especially to decipher the thermoregulatory strategies of extinct terrestrial vertebrates, mainly reptiles. Cretaceous latitudinal thermal gradients were however partly reconstructed on the basis of a uniformitarian approach, by comparing the occurrence and distribution of fossil vertebrate assemblages with that of their nearest present-day relatives [11,12] and by studying fossil plant distribution and physiognomy [13–15]. Weak latitudinal temperature gradients during the Cretaceous were deduced from the distribution of paleobotanical and geochemical data mentioned above [16].

The aim of this study is to propose a temperature gradient from 80°N to 30°S for the Late Campanian–Middle Maastrichtian interval by using the oxygen isotope compositions of continental vertebrate phosphatic tissues as proxies of mean air temperatures. A present-day transfer function is established between vertebrate <sup>18</sup>O values, meteoric water <sup>18</sup>O values and mean air temperatures. It is applied to published and 19 new <sup>18</sup>O data from well-preserved reptile phosphatic remains (mainly tooth enamel from dinosaurs and crocodylians and dense bone from turtle plates) recovered from deposits for which paleolatitudes are calculated from paleogeographic and paleomagnetic data.

The restored latitudinal thermal gradient for the Late Campanian–Middle Maastrichtian is discussed regarding the following points:

- (1) original versus diagenetic oxygen isotope record;
- (2) compatibility with other gradients derived from paleontological proxies;
- (3) comparison with the published marine thermal gradients and the possible existence of polar ice; and
- (4) relation to the latitudinal distribution of continental vertebrates.

## 2. Methods

Late Campanian to Middle Maastrichtian vertebrates are assumed to have drunk local water or ingested water in plants or meat that was derived from rainfall. Therefore, the oxygen isotope composition of apatite from Late Campanian–Middle Maastrichtian reptiles can potentially be used as a proxy of contemporaneous meteoric water <sup>18</sup>O values, hence of variations in mean air temperatures with latitude [17]. To perform these calculations, present-day reference equations that relate the three following parameters are needed: (1) the <sup>18</sup>O values of vertebrate phosphate, (2) the <sup>18</sup>O values of meteoric water and 3) the mean air temperature.

Mean annual air temperatures and <sup>18</sup>O values of weighted meteoric waters are calculated from monthly averages of data provided by the global network of weather stations operated by the IAEA–WMO (International Atomic Energy Agency–World Meteorological Organization, [18]). Because Upper Campanian–Middle Maastrichtian studied sampling sites were located in the vicinity of coast lines (Fig. 1), the computed reference equations must be established with present-day <sup>18</sup>O values of meteoric water and mean air temperatures recalculated at sea level. For weather stations that are located at higher altitudes, data were corrected by subtracting 0.3‰ and 0.5 °C per 100 m of elevation [19]. These weighted <sup>18</sup>O values of meteoric waters from IAEA–WMO stations are plotted against the absolute latitude values in Fig. 2 (curve 1). The resulting computed Eq. (1) is comparable to the equation previously proposed by Bowen and Wilkinson [20].

Present-day apatite <sup>18</sup>O values between 0° and 80° in latitude are calculated using fractionation equations

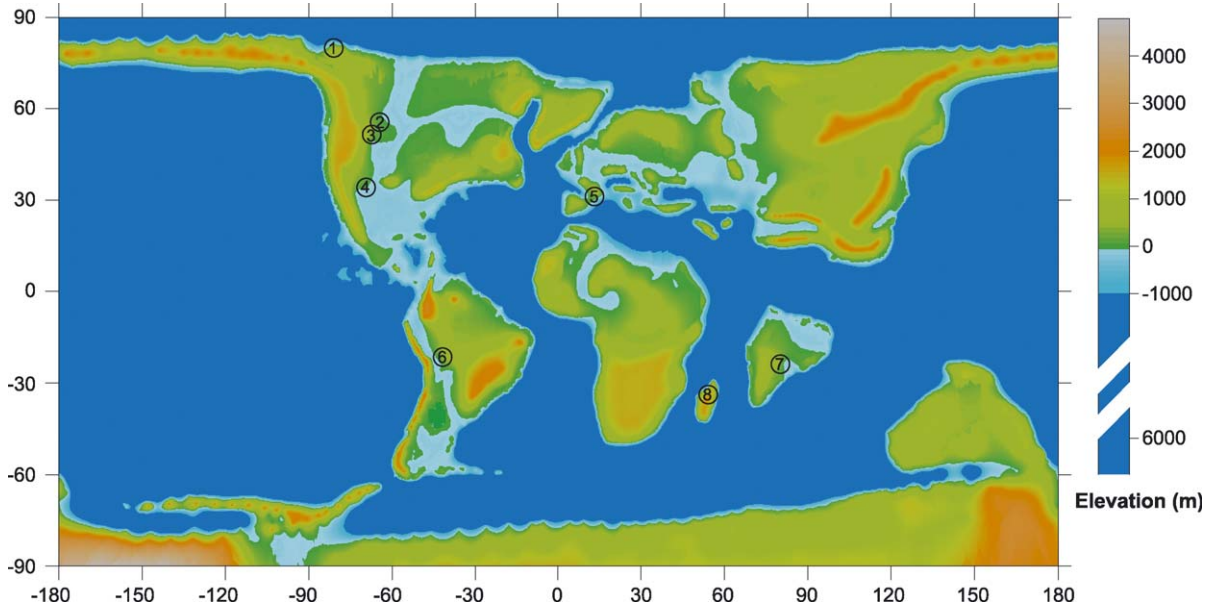


Fig. 1. Late Campanian–Middle Maastrichtian paleogeographic map showing the location of sites where vertebrate remains used for the geochemical analyses described in the present paper have been collected.

of turtles [21], freshwater fish [22] and mammals for all IAEA–WMO meteorological stations around the world that provide both rainfall  $\delta^{18}\text{O}$  values and mean annual air temperatures (Fig. 2). Although the debate about dinosaur physiology is still largely open (e.g., [23–26]), it is frequently supposed that while Cretaceous crocodylians certainly had the same poikilothermic metabolism as their living counterparts, dinosaurs were largely homeothermic [27]. Therefore, a general oxygen isotope fractionation equation is also calculated for present-day homeotherms (mammals) on the basis of a compilation of data published in the literature (see Annex 1).

An oxygen isotope latitudinal gradient based on phosphate  $\delta^{18}\text{O}$  values of vertebrates is then obtained and reflects variations in meteoric water  $\delta^{18}\text{O}$  values (Fig. 2), themselves closely related to mean annual air temperatures [28,29]. The model apatite  $\delta^{18}\text{O}$  values define a larger envelope than that for meteoric water  $\delta^{18}\text{O}$  values from which they derive because they result from the simultaneous application of fractionation equations corresponding to turtles, fish and mammals (Fig. 2). Curves (1) and (2) obtained by polynomial regression of meteoric water and vertebrate  $\delta^{18}\text{O}$  values have a similar slope; however, the intercept for the

vertebrate curve (2) is about 21.9‰ higher than for the meteoric water curve (1),

$$\delta^{18}\text{O}_{\text{meteoric water}} = -0.0058L^2 + 0.1172L - 3.321 \quad (1)$$

$$\delta^{18}\text{O}_{\text{apatite}} = -0.0051L^2 + 0.1170L - 18.578 \quad (2)$$

where  $L$  is the latitude. This result is explained by an  $^{18}\text{O}$  enrichment of the animal's body water and phosphatic tissues relative to surface waters, a consequence of its general metabolism, temperature and the oxygen isotope fractionation between biogenic apatite and body water [30,31]. For internal consistency, using the same meteorological data set, the following linear relationship between  $\delta^{18}\text{O}_{\text{meteoric water}}$  and mean annual air temperatures is obtained (Fig. 3),

$$\delta^{18}\text{O}_{\text{water}} = (0.49 \pm 0.03)T - (14.18 \pm 0.52) \quad (3)$$

and does not differ significantly from previously published equations [29,32].

Assuming that Eq. (3) can be applied to the Late Campanian–Middle Maastrichtian, the reconstruction of the latitudinal thermal gradient is performed through the following steps:

- calculation of sampling site paleolatitudes,

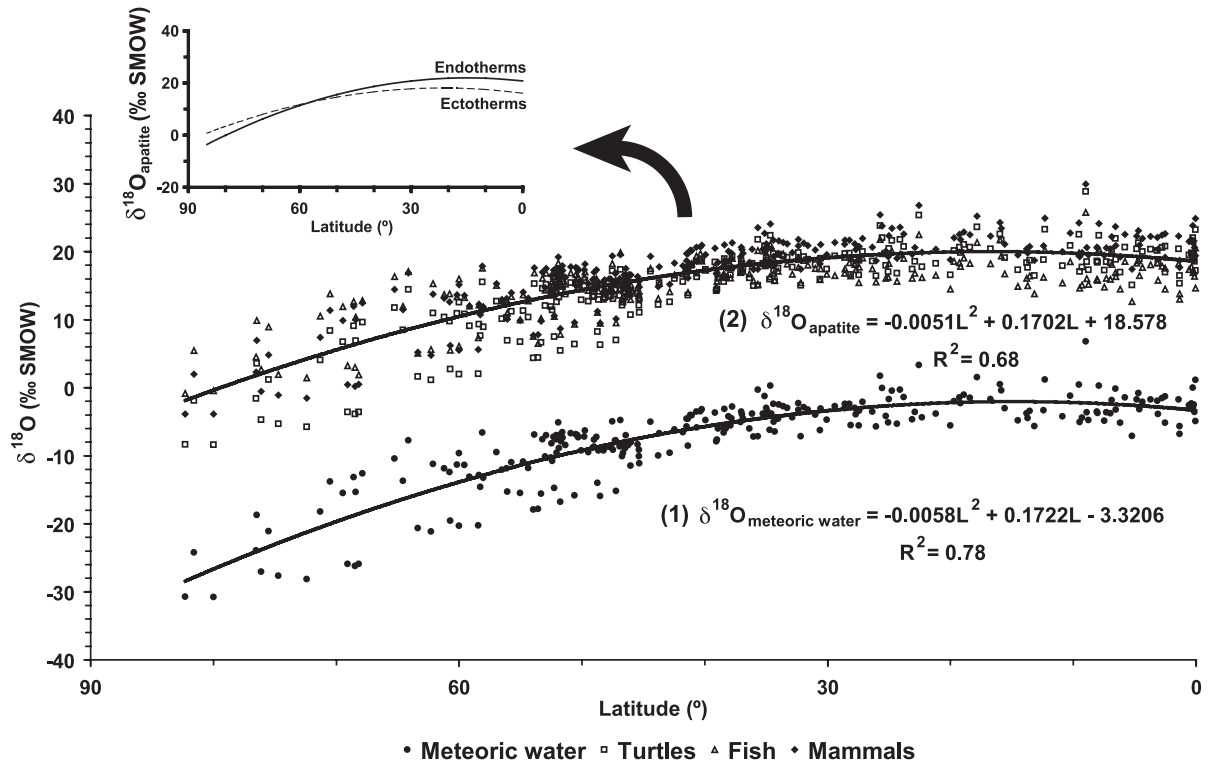


Fig. 2. Present-day  $\delta^{18}\text{O}$  values of meteoric waters and vertebrate phosphate (mammals, fish and turtles) as a function of absolute latitude values. Vertebrate phosphate  $\delta^{18}\text{O}$  values are calculated using the following empirical fractionation equations:

$$\delta^{18}\text{O}_{\text{water}} = 1.11\delta^{18}\text{O}_{\text{mammals}} - 26.44 \quad (\text{this study; see Annex 1}) \quad (\text{a})$$

$$T(^{\circ}\text{C}) = -4.38(\delta^{18}\text{O}_{\text{fish}} - \delta^{18}\text{O}_{\text{water}}) + 113.3 \quad [22]. \quad (\text{b})$$

$$\delta^{18}\text{O}_{\text{water}} = 1.01\delta^{18}\text{O}_{\text{turtle}} - 22.3 \quad [21] \quad (\text{c})$$

Polynomial regression curves (1) and (2) were computed for all meteoric water and vertebrate  $\delta^{18}\text{O}$  data, respectively. The upper left inset shows how  $\delta^{18}\text{O}$  values of endotherms and ectotherms differ as a function of latitude as a consequence of their body temperature differences.

- estimation of past meteoric water  $\delta^{18}\text{O}$  values by subtracting the intercept difference of 21.9 between Eqs. (1) and (2) from new and published (Table 1)  $\delta^{18}\text{O}$  values of fossil vertebrates [21,33,34],
- calculation of past mean air temperatures by using Eq. (3).

Calculation of sampling site geographic coordinates was made by moving plates into their paleo-positions using the method described by Besse and Courtillot [35]. The oceanic kinematic parameters are used to arrange the major continents into their relative

positions (Fig. 1). The Apparent Polar Wander Paths (APWP) of continents calculated by Besse and Courtillot [36,37] and Chen et al. [38] are then used to set out the paleolatitude grid. These APWP were constructed using a selection of the best paleomagnetic poles available for Eurasia, North America, South America and Western and South Africa which were averaged over 10-My time windows (except Western Africa, which was averaged over a 20-My time window). In order to reconstruct the latitudinal thermal gradient, only paleolatitudes and associated uncertainties are shown in Table 1. These uncertain-

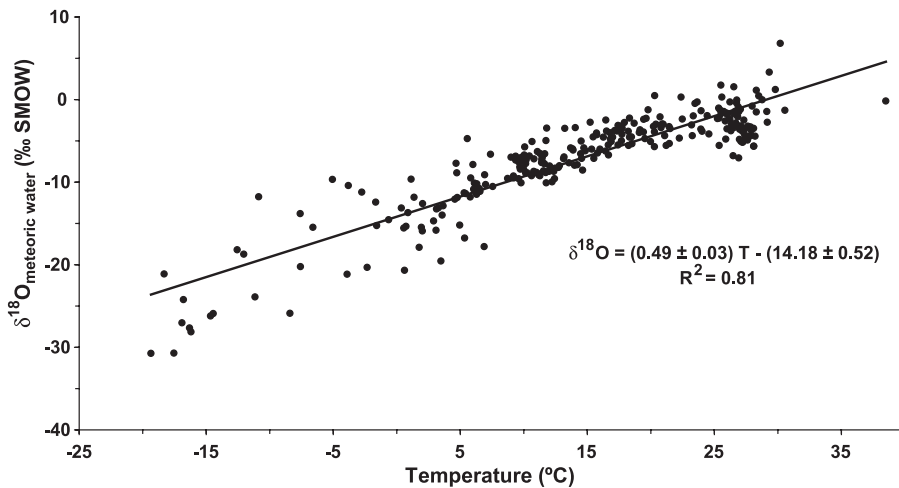


Fig. 3. Meteoric water  $\delta^{18}\text{O}$  values reported as a function of mean annual air temperatures. Mean annual air temperature and weighted meteoric water  $\delta^{18}\text{O}$  values are calculated from monthly averages of data provided by the global network of weather stations operated by the IAEA–WMO (International Atomic Energy Agency–World Meteorological Organization). Because living altitudes are generally not known in the case of paleoclimatic reconstructions, data have been recalculated on the sea-level baseline by using the following corrections: 0.3‰ and 0.5 °C per 100 m of elevation [94]. Uncertainties associated with the slope and intercept of the regression line correspond to  $2\sigma$  standard deviations.

ties depend on the quality and number of magnetic poles used to build the APWP.

### 3. Sample collection

The 19 phosphatic remains analyzed for their oxygen isotope compositions were collected as isolated specimens (shed teeth, broken turtle shell fragments and isolated fish scales). The sampled localities were recovered from various paleolatitudes that can be considered as roughly contemporaneous, within the dating uncertainties inherent to nonmarine formations for which no radiometric ages are available. The Campanian–Maastrichtian boundary is placed at  $72.0 \pm 0.5$  Ma [39].

All studied samples come from deposits of reasonably well known age. The French locality of Cruzy (Hérault) can be considered to be Late Campanian–Early Maastrichtian in age [40]. The North American locality near Onefour (Alberta) is known to be Late Campanian in age [41] and the Pajcha Pata locality (Bolivia) was dated to Middle Maastrichtian [42]. Depending on the tooth size, enamel or bulk tooth was analyzed (Table 1). When the tooth was large enough, enamel was sampled along the tooth with a microdrill. As crocodile teeth need several months (between 6

months and 1 year) to complete their growth, enamel was sampled from the base of the crown to the apex in order to avoid possible seasonal  $\delta^{18}\text{O}$  variations. In the case of turtles, only compact bone from the shell was sampled. Enamel from the scales of gar-like fishes was mechanically isolated under a binocular microscope.

### 4. Analytical techniques

Measurements of oxygen isotope ratios of apatite consist of isolating  $\text{PO}_4^{3-}$  using acid dissolution and anion-exchange resin, according to a protocol derived from the original method published by Crowson et al. [43] and slightly modified by Lécuyer et al. [44]. Silver phosphate is quantitatively precipitated in a thermostatic bath set at a temperature of 70 °C. After filtration, washing with double deionised water and drying at 50 °C, 15 mg of  $\text{Ag}_3\text{PO}_4$  are mixed with 0.8 mg of pure powder graphite.  $^{18}\text{O}/^{16}\text{O}$  ratios are measured by reducing silver phosphates to  $\text{CO}_2$  using graphite reagent [45,46]. Samples are weighed into tin reaction capsules and loaded into quartz tubes and degassed for 30 min at 80 °C under vacuum. Each sample was heated at 1100 °C for 1 min to promote the redox reaction. The  $\text{CO}_2$  produced was directly trapped in

Table 1

Oxygen isotope compositions of phosphate from Late Campanian–Middle Maastrichtian vertebrates measured in this study and compiled from the literature

Sample	Taxon	Sample nature	Location	Stratigraphic age	$\delta^{18}\text{O}$ (PO <sub>4</sub> ) ‰ (SMOW)	Paleolatitude (°)	Error –	Error +	Source
Theropod-1	<i>Albertosaurus</i>		Alaska	Upper Campanian	10.2	83.3	3.8	9.3	Fricke and Rogers [34]
Theropod-2	<i>Albertosaurus</i>		Alaska	Upper Campanian	9.8	83.3	3.8	9.3	Fricke and Rogers [34]
Theropod-3	<i>Albertosaurus</i>		Alaska	Upper Campanian	10.4	83.3	3.8	9.3	Fricke and Rogers [34]
Theropod-4	<i>Albertosaurus</i>		Alaska	Upper Campanian	10.2	83.3	3.8	9.3	Fricke and Rogers [34]
–	Hadrosauridae		Alaska	Upper Campanian	6.45	83.3	3.8	9.3	Kolodny et al. [33]
–	Bony fish		Alaska	Upper Campanian	8.0	83.3	3.8	9.3	Kolodny et al. [33]
CA001	Theropoda	Tb	Alberta	Upper Campanian	11.9	58.6	8.1	7.2	This study
CA010	Ornithopoda	Te	Alberta	Upper Campanian	13.9	58.6	8.1	7.2	This study
CA004	Crocodylian	Te	Alberta	Upper Campanian	12.0	58.6	8.1	7.2	This study
CA006	Turtle	bone	Alberta	Upper Campanian	14.8	58.6	8.1	7.2	This study
CA003	Lepisosteidae	scale	Alberta	Upper Campanian	12.0	58.6	8.1	7.2	This study
Theropod-1	<i>Albertosaurus</i>		Alberta	Upper Campanian	11.6	58.6	8.1	7.2	Fricke and Rogers [34]
Theropod-2	<i>Albertosaurus</i>		Alberta	Upper Campanian	13.2	58.6	8.1	7.2	Fricke and Rogers [34]
Theropod-3	<i>Albertosaurus</i>		Alberta	Upper Campanian	12.6	58.6	8.1	7.2	Fricke and Rogers [34]
Theropod-4	<i>Albertosaurus</i>		Alberta	Upper Campanian	13.0	58.6	8.1	7.2	Fricke and Rogers [34]
Theropod-5	<i>Albertosaurus</i>		Alberta	Upper Campanian	13.4	58.6	8.1	7.2	Fricke and Rogers [34]
Crocodyle-1	Crocodylian		Alberta	Upper Campanian	13.9	58.6	8.1	7.2	Fricke and Rogers [34]
Crocodyle-2	Crocodylian		Alberta	Upper Campanian	13.6	58.6	8.1	7.2	Fricke and Rogers [34]
Crocodyle-3	Crocodylian		Alberta	Upper Campanian	14.6	58.6	8.1	7.2	Fricke and Rogers [34]
Crocodyle-4	Crocodylian		Alberta	Upper Campanian	14.7	58.6	8.1	7.2	Fricke and Rogers [34]
–	<i>Aspideretes</i>		Alberta	Upper Campanian	12.7	58.6	8.1	7.2	Barrick et al. [21]
–	<i>Aspideretes</i>		Alberta	Upper Campanian	12.1	58.6	8.1	7.2	Barrick et al. [21]
–	<i>Aspideretes</i>		Alberta	Upper Campanian	11.6	58.6	8.1	7.2	Barrick et al. [21]
–	<i>Aspideretes</i>		Alberta	Upper Campanian	11.5	58.6	8.1	7.2	Barrick et al. [21]
–	<i>Aspideretes</i>		Alberta	Upper Campanian	10.6	58.6	8.1	7.2	Barrick et al. [21]
–	Lepisosteidae		Alberta	Upper Campanian	12.1	58.6	8.1	7.2	Barrick et al. [21]
–	Lepisosteidae		Alberta	Upper Campanian	12.0	58.6	8.1	7.2	Barrick et al. [21]
–	Lepisosteidae		Alberta	Upper Campanian	11.9	58.6	8.1	7.2	Barrick et al. [21]

Table 1 (continued)

Sample	Taxon	Sample nature	Location	Stratigraphic age	$\delta^{18}\text{O}$ (PO4) ‰ (SMOW)	Paleolatitude (°)	Error –	Error +	Source
–	Lepisosteidae		Alberta	Upper Campanian	11.4	58.6	8.1	7.2	Barrick et al. [21]
–	Lepisosteidae		Alberta	Upper Campanian	11.5	58.6	8.1	7.2	Barrick et al. [21]
–	Lepisosteidae		Alberta	Upper Campanian	11.1	58.6	8.1	7.2	Barrick et al. [21]
–	Lepisosteidae		Alberta	Upper Campanian	10.9	58.6	8.1	7.2	Barrick et al. [21]
Theropod-1	<i>Albertosaurus</i>		Montana	Campanian	12.9	54.8	7.6	6.8	Fricke and Rogers [34]
Theropod-2	<i>Albertosaurus</i>		Montana	Campanian	12.5	54.8	7.6	6.8	Fricke and Rogers [34]
Theropod-3	<i>Albertosaurus</i>		Montana	Campanian	13.5	54.8	7.6	6.8	Fricke and Rogers [34]
Theropod-4	<i>Albertosaurus</i>		Montana	Campanian	13.1	54.8	7.6	6.8	Fricke and Rogers [34]
Theropod-5	<i>Albertosaurus</i>		Montana	Campanian	14.8	54.8	7.6	6.8	Fricke and Rogers [34]
Theropod-6	<i>Albertosaurus</i>		Montana	Campanian	11.8	54.8	7.6	6.8	Fricke and Rogers [34]
Theropod-7	<i>Albertosaurus</i>		Montana	Campanian	15.4	54.8	7.6	6.8	Fricke and Rogers [34]
Theropod-8	<i>Albertosaurus</i>		Montana	Campanian	14.1	54.8	7.6	6.8	Fricke and Rogers [34]
Crocodile-1	Crocodylian		Montana	Campanian	14.7	54.8	7.6	6.8	Fricke and Rogers [34]
Crocodile-2	Crocodylian		Montana	Campanian	16.2	54.8	7.6	6.8	Fricke and Rogers [34]
Crocodile-3	Crocodylian		Montana	Campanian	15.4	54.8	7.6	6.8	Fricke and Rogers [34]
Crocodile-4	Crocodylian		Montana	Campanian	14.1	54.8	7.6	6.8	Fricke and Rogers [34]
Crocodile-5	Crocodylian		Montana	Campanian	14.7	54.8	7.6	6.8	Fricke and Rogers [34]
Crocodile-6	Crocodylian		Montana	Campanian	15.0	54.8	7.6	6.8	Fricke and Rogers [34]
Crocodile-7	Crocodylian		Montana	Campanian	14.9	54.8	7.6	6.8	Fricke and Rogers [34]
Crocodile-8	Crocodylian		Montana	Campanian	13.4	54.8	7.6	6.8	Fricke and Rogers [34]
Crocodile-9	Crocodylian		Montana	Campanian	14.1	54.8	7.6	6.8	Fricke and Rogers [34]
Theropod-1	<i>Saurornitholestes</i>		Texas	U. Campan.–L. Maastr.	17.0	36.0	5.2	4.6	Fricke and Rogers [34]
Theropod-2	<i>Saurornitholestes</i>		Texas	U. Campan.–L. Maastr.	18.3	36.0	5.2	4.6	Fricke and Rogers [34]
Theropod-4	<i>Saurornitholestes</i>		Texas	U. Campan.–L. Maastr.	17.5	36.0	5.2	4.6	Fricke and Rogers [34]
Crocodile-1	Crocodylian		Texas	U. Campan.–L. Maastr.	16.8	36.0	5.2	4.6	Fricke and Rogers [34]

(continued on next page)

Table 1 (continued)

Sample	Taxon	Sample nature	Location	Stratigraphic age	$\delta^{18}\text{O}$ (PO4) ‰ (SMOW)	Paleolatitude (°)	Error –	Error +	Source
Crocodile-2	Crocodylian		Texas	U. Campan.–L. Maastr.	17.1	36.0	5.2	4.6	Fricke and Rogers [34]
Crocodile-3	Crocodylian		Texas	U. Campan.–L. Maastr.	16.7	36.0	5.2	4.6	Fricke and Rogers [34]
Crocodile-4	Crocodylian		Texas	U. Campan.–L. Maastr.	16.7	36.0	5.2	4.6	Fricke and Rogers [34]
–	Crocodylian		Texas	Campanian	17.7	36.0	5.2	4.6	Kolodny et al. [33]
–	Carnosaurian		Texas	Campanian	17.3	36.0	5.2	4.6	Kolodny et al. [33]
–	Ceratopsian		Texas	Campanian	17.2	36.0	5.2	4.6	Kolodny et al. [33]
–	Turtle		Texas	Campanian	18.4	36.0	5.2	4.6	Kolodny et al. [33]
F001	<i>Tarascosaurus salluvicus</i>	Te	France	U. Campan.–L. Maastr.	20.7	35.5	5.2	4.6	This study
F002	<i>Tarascosaurus salluvicus</i>	Te	France	U. Campan.–L. Maastr.	19.4	35.5	5.2	4.6	This study
F003	<i>Rabdodon priscus</i>	Tb	France	U. Campan.–L. Maastr.	18.0	35.5	5.2	4.6	This study
F004	<i>Rabdodon priscus</i>	Te	France	U. Campan.–L. Maastr.	18.9	35.5	5.2	4.6	This study
F028	<i>Ampelosaurus atacis</i>	Tb	France	U. Campan.–L. Maastr.	18.8	35.5	5.2	4.6	This study
F005	Crocodylian	Te	France	U. Campan.–L. Maastr.	18.6	35.5	5.2	4.6	This study
F026	Crocodylian	Tb	France	U. Campan.–L. Maastr.	17.5	35.5	5.2	4.6	This study
F007	cf. Foxemys	bone	France	U. Campan.–L. Maastr.	17.6	35.5	5.2	4.6	This study
F029	cf. Foxemys	bone	France	U. Campan.–L. Maastr.	17.5	35.5	5.2	4.6	This study
F030	cf. Foxemys	bone	France	U. Campan.–L. Maastr.	16.8	35.5	5.2	4.6	This study
F006	Lepisosteidae	scale	France	U. Campan.–L. Maastr.	17.6	35.5	5.2	4.6	This study
PM122	Crocodylian	Tb	Bolivia	Middle Maastrichtian	19.1	–19.6	2.3	2.5	This study
PM122-1	Crocodylian	Tb	Bolivia	Middle Maastrichtian	20.1	–19.6	2.3	2.5	This study
PM122-2	Crocodylian	Tb	Bolivia	Middle Maastrichtian	20.4	–19.6	2.3	2.5	This study
Crocodile-1	Crocodylian		India	Maastrichtian	17.2	–23.7	2.9	3.1	Fricke and Rogers [34]
Crocodile-2	Crocodylian		India	Maastrichtian	17.0	–23.7	2.9	3.1	Fricke and Rogers [34]
Crocodile-3	Crocodylian		India	Maastrichtian	16.6	–23.7	2.9	3.1	Fricke and Rogers [34]
Theropod-1	<i>Majungatholus</i>		Madagascar	Lower Maastrichtian	21.6	–32.0	3.2	3.5	Fricke and Rogers [34]



Table 1 (continued)

Sample	Taxon	Sample nature	Location	Stratigraphic age	$\delta^{18}\text{O}$ (PO4) ‰ (SMOW)	Paleolatitude (°)	Error –	Error +	Source
Theropod-2	<i>Majungatholus</i>		Madagascar	Lower Maastrichtian	23.2	–32.0	3.2	3.5	Fricke and Rogers [34]
Theropod-3	<i>Majungatholus</i>		Madagascar	Lower Maastrichtian	23.2	–32.0	3.2	3.5	Fricke and Rogers [34]
Theropod-4	<i>Majungatholus</i>		Madagascar	Lower Maastrichtian	20.2	–32.0	3.2	3.5	Fricke and Rogers [34]
Theropod-5	<i>Majungatholus</i>		Madagascar	Lower Maastrichtian	19.6	–32.0	3.2	3.5	Fricke and Rogers [34]
Crocodile-1	Crocodylian		Madagascar	Lower Maastrichtian	20.2	–32.0	3.2	3.5	Fricke and Rogers [34]
Crocodile-2	Crocodylian		Madagascar	Lower Maastrichtian	21.2	–32.0	3.2	3.5	Fricke and Rogers [34]
Crocodile-3	Crocodylian		Madagascar	Lower Maastrichtian	21.1	–32.0	3.2	3.5	Fricke and Rogers [34]

Taxons, locations, stratigraphic ages and data sources are reported along with calculated paleolatitudes and their associated uncertainties.

liquid nitrogen to avoid any kind of isotopic reaction with quartz at high temperature.  $\text{CO}_2$  was then analyzed with a Finnigan DeltaE™ mass spectrometer at the Laboratory UMR CNRS 5125 ‘PEPS’, University Claude Bernard Lyon 1. Isotopic compositions are quoted in the standard  $\delta$  notation relative to V-SMOW. Silver phosphate precipitated from standard NBS120c (natural Miocene phosphorite from Florida) was repeatedly analyzed ( $\delta^{18}\text{O}=21.67\pm 0.18$ ;  $n=15$ ) along with the silver phosphate samples derived from the Late Campanian–Middle Maastrichtian vertebrate remains.

## 5. Results and discussion

Oxygen isotope compositions of vertebrate phosphates measured in this study or compiled from the literature are shown in Table 1 and plotted as a function of latitude in Fig. 4. Taking into account the uncertainties associated with both the variability in  $\delta^{18}\text{O}$  values of vertebrates and the latitudinal position of Late Campanian–Middle Maastrichtian plates, the computed curve for the isotopic gradient has a lower slope than for the present. It is noteworthy that the influence of oceanic currents on the temperature versus latitude relationship cannot be evaluated for those studied sites which were close to the coast lines. We can question whether this isotopic record is primary or partly results from a diagenetic alteration of studied fossil biogenic phosphates.

### 5.1. Did fossil vertebrates preserve their original isotope composition?

Secondary precipitation of apatite and isotopic exchange during microbially mediated reactions may scramble the primary isotopic signal [47,48]. However, apatite crystals that make up tooth enamel are large and densely packed, and isotopic exchange under inorganic conditions has little effect on the oxygen isotope composition of phosphates even at geological time scales [22,49]. We emphasize that tooth enamel remains the best biomineral to reconstruct Pre-Cenozoic air or marine temperatures, as illustrated by several case studies [7,50–52]. Although no method is available to demonstrate definitively whether diagenetic processes may have affected oxygen isotope compositions of bulk tooth phosphate, several considerations support the probable preservation of pristine isotopic signals (Table 1).

- (1) As previously noted by Fricke et al. [53], Fricke and Rogers [34] and illustrated in Fig. 2, body temperature differences between ectotherms and endotherms result in different  $\delta^{18}\text{O}$  values of apatite phosphate as a function of latitude. They are characterized by higher values for ectotherms than for endotherms at high latitudes (due to lower body temperature for ectotherms), and conversely, higher  $\delta^{18}\text{O}$  values for endotherms at low latitudes. Using this relationship, these authors observed a similar isotopic differ-

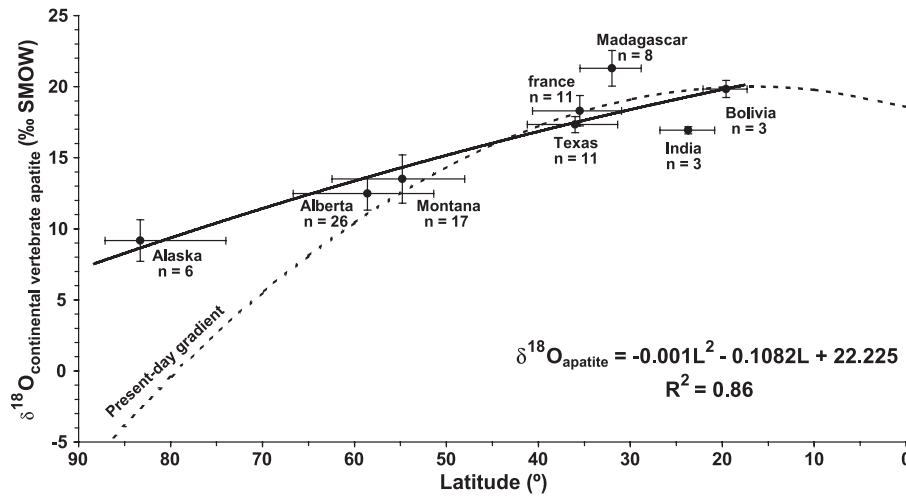


Fig. 4. Mean vertebrate phosphate  $\delta^{18}\text{O}$  values plotted against absolute paleolatitudes of sampled sites. Present-day vertebrate  $\delta^{18}\text{O}$  gradient, illustrated in Fig. 2 (polynomial regression curve 2), is given for comparison. Oxygen isotope data and paleolatitudes along with uncertainties are from Table 1. The label ‘ $n$ ’ corresponds to the number of analyzed vertebrate specimens at each geographic site.

ence between theropod dinosaurs and crocodiles and therefore assumed a thermophysiological difference, the theropods being supposedly more endothermic [34]. Diagenetic processes are expected to modify and homogenise  $\delta^{18}\text{O}$  values of both endotherms and ectotherms after isotopic exchange between apatite and local groundwater (see [51]). Therefore, systematic differences in the oxygen isotope compositions observed between dinosaurs, freshwater crocodiles and turtles provide a good indicator of preservation. Adding our data to those published by Fricke and Rogers [34], this physiological record seems to be confirmed (Fig. 5) despite (i) the large isotopic variability of fossil vertebrates at each site, (ii) uncertainties in paleolatitudes and (iii) the lack of data for “crocodile–dinosaur pairs” at very low latitudes. Although the two computed regression lines for Late Campanian–Middle Maastrichtian endotherms and ectotherms intersect at a paleolatitude of  $50^\circ$  (Fig. 5), similar to the present-day modeled curves shown in Fig. 2, we emphasize that these two regression lines have slopes and intercepts that are not statistically different.

(2) For some studied sites (Texas, France and Madagascar), there are no significant oxygen isotope differences between fossil endotherms and ectotherms (Fig. 5). In a recent study devoted

to the oxygen isotope compositions of Maastrichtian vertebrate phosphatic remains (dinosaur, turtles, crocodiles and fish) from Laño, Spain, Lécuyer et al. [51] did not find any expected ecological or physiological  $\delta^{18}\text{O}$  difference between the various taxa and therefore concluded that these values result from early diagenetic processes. In this case, the isotopic compositions only reflect the local climate during the deposition of the vertebrate-bearing sediments. Accordingly, we cannot exclude that some studied Late Campanian–Middle Maastrichtian vertebrate remains from the above-mentioned sites may have suffered from late and extensive diagenetic processes [33].

(3) Intra-tooth oxygen isotope time series have been obtained from the enamel phosphate of dinosaurs [54]. The isotopic patterns that mimic sinusoidal-like seasonal variations are interpreted as recording the Campanian–Maastrichtian climatic seasonality at high latitudes (Alberta, Canada). These results confirm that tooth enamel from continental vertebrates of Cretaceous age may constitute a valuable material to restore paleoclimates.

(4) Another way to test the reliability of the reconstructed thermal gradient based on vertebrate  $\delta^{18}\text{O}$  values is to compare it with other climatic proxies. Wolfe and Upchurch [13]

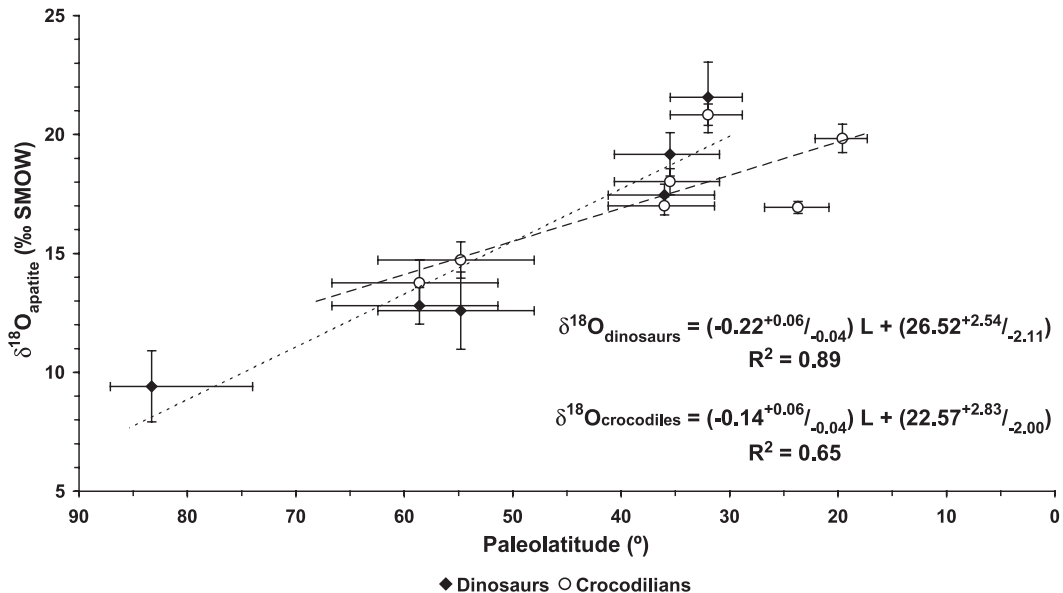


Fig. 5. Latitudinal distribution of dinosaur and crocodile apatite  $\delta^{18}\text{O}$  values. Despite a large natural oxygen isotope variability among vertebrate specimens at each sampled site, crocodiles have higher  $\delta^{18}\text{O}$  values than dinosaurs above  $50^\circ$  of paleolatitude, a tendency that is reversed at low latitudes. This isotopic pattern, interpreted as resulting from body temperature differences, resembles the present-day oxygen isotope latitudinal distribution between ectotherms and endotherms (Fig. 2). As data are not normally distributed, bootstrapped 95% confidence intervals for the slope and intercept were calculated using 'PAST' software [95].

compared the physiognomy (including leaf-margin analysis) of North American fossil floras (ranging in age from the Early Cretaceous to the Eocene) with extant equivalents and proposed a mean air temperature of about  $22^\circ\text{C}$  for the Early Maastrichtian of southeastern North America (paleolatitude  $\sim 30^\circ\text{N}$ ). Using the same method, mean air temperatures during the Campanian and Maastrichtian were estimated to be  $5 \pm 3^\circ\text{C}$  for the North Slope of Alaska ( $75\text{--}80^\circ\text{N}$ ) [13] and  $13^\circ\text{C}$  for the Antarctic Peninsula ( $\sim 60^\circ\text{S}$ ) [15]. Kennedy et al. [55] proposed a temperature range of  $12\text{--}15^\circ\text{C}$  for the northwest of the South Island, New Zealand ( $50\text{--}60^\circ\text{S}$ ). These temperatures are close to those calculated from  $\delta^{18}\text{O}$  values of vertebrates (Fig. 6). Moreover, at low latitudes, estimated mean air temperatures of about  $25^\circ\text{C}$ , which are inferred from Late Campanian–Middle Maastrichtian  $\delta^{18}\text{O}$  values of vertebrates, are also similar to Sea Surface Temperatures (SST) calculated from oxygen isotope compositions of foraminifera or fish tooth enamel [7,56–59].

Considering that various climatic proxies provide comparable temperatures to those obtained from  $\delta^{18}\text{O}$  values of vertebrates, we propose that the distribution of these latter as a function of paleolatitudes could constitute a valuable proxy of the Late Campanian–Middle Maastrichtian continental thermal gradient.

### 5.2. Implications for global climate during the Late Campanian–Middle Maastrichtian

The Late Campanian–Middle Maastrichtian temperature gradient mimics the present-day one from the equator to  $30^\circ$ , then decreases toward the poles with a slope of about  $0.4 \pm 0.1^\circ\text{C}/^\circ\text{latitude}$  instead of  $0.6^\circ\text{C}/^\circ\text{latitude}$  for the present. According to this gradient, freezing conditions were probably reached above  $80^\circ$  of latitude, with a mean polar temperature of about  $-5^\circ\text{C}$ .

A high  $\text{CO}_2$  atmospheric content associated with an enhanced oceanic heat transport were proposed to explain a flat equator-to-pole thermal gradient [60–62]. A weak gradient at both sea and air surfaces should reduce the atmospheric and oceanic circula-

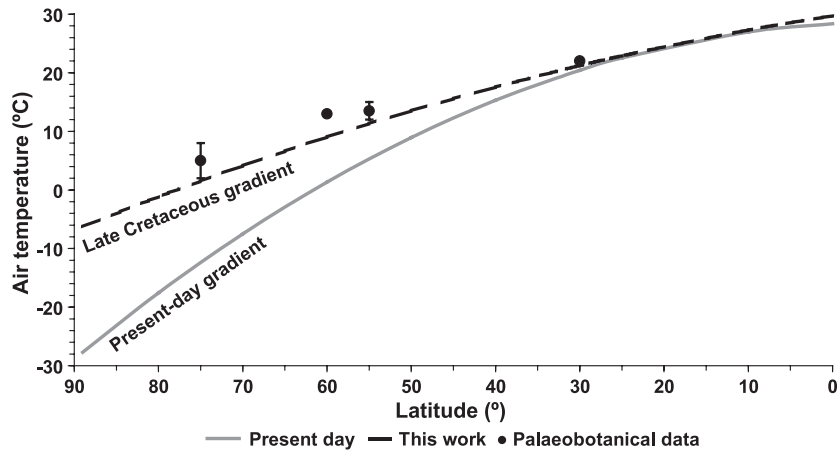


Fig. 6. Computed mean annual temperatures during the Campanian–Maastrichtian versus absolute latitudes. The Late Campanian–Middle Maastrichtian thermal gradient was calculated using fossil vertebrate  $\delta^{18}\text{O}$  values and Eqs. (1)–(3) [see text for details]. Air temperature estimates from plant physiognomy [13–15,55] are plotted as black dots and fall close to the thermal gradient proposed in this study. The present-day continental temperature gradient is given for comparison.

tions. However, a flat thermal gradient is actually linked to a warming at high latitudes, thus altering the Earth's radiative budget, the albedo (less perennial snow, presence of forest at high latitudes) as well as the cloud cover. This mechanism limits the weakening of the atmospheric circulation and therefore moderates the warming at the tropics without avoiding a significant cooling generally observed at mid-latitudes in the central areas of largest continents. Using an oceanic general circulation model, Brady et al. [63] and DeConto et al. [64] suggest that a strong equator-to-pole oceanic heat transport, limiting the warming at low latitudes, could be maintained when the thermal gradient is flat. The two main reasons invoked are the strengthening of the ocean meridional overturning and the reduction of the wind-driven oceanic circulation.

According to Wolfe and Upchurch [13], equability can be defined as the mean annual range of temperature with a higher equability implying a lower mean annual range of temperatures. They proposed for the Campanian a mean annual range temperature of 12 to 20 °C at a paleolatitude of 52–55°N and an extrapolated value of –2 to 8 °C at the poles.

This thermal seasonality may explain a part of the vertebrate oxygen isotope variability observed within each sampling site (Fig. 4). Oxygen isotope measurements from Madagascar and India fall above and below the computed latitudinal thermal gradient (Fig.

4). It must be kept in mind that the amount of precipitation can influence the  $\delta^{18}\text{O}$  values of rain, especially at low latitudes, and thereby the  $\delta^{18}\text{O}$  values of vertebrates. In the case of a dry climate with low seasonal rainfall, water sources for vertebrates can be subjected to high evaporation effects. The resulting high  $\delta^{18}\text{O}$  values of vertebrates potentially lead to overestimate air temperatures. Moreover, skeletal phosphate from some reptiles such as the extant snake *Cerastes vipera* from the Sahara desert has very high  $\delta^{18}\text{O}$  values of 30‰ that are explained by peculiar water-keeping strategies [65]. Conversely, high amounts of precipitation may lead to underestimate air temperatures.

It is likely, however, that most of the studied Late Campanian–Middle Maastrichtian locations did not suffer such extreme conditions. Indeed, on the basis of plant physiognomy (wood growth rings and leaf morphology), precipitation parameters can be estimated. For example, North American climates were characterized by low-to-moderate amounts of precipitations well distributed throughout the year at low-to-middle latitudes, increasing and becoming somewhat seasonal above paleolatitudes of 45–50° [13]. North American temperate climates could result from the presence of the Western Interior Seaway (Fig. 1). Using the Climate Leaf Analysis Multivariate Program (CLAMP, [66]), the Late Cretaceous floras of the South Island, New Zealand (paleolatitude about 60°S),

indicate a temperate regional climate with significant rainfall and mean annual temperatures in the range 12–15 °C [55].

At high latitudes, paleotemperatures are estimated to be from 15 to 25 °C higher than modern ones. However, considering possible freezing conditions and a relatively high thermal equability ( $T$  from –10 to 0 °C) deduced from both our data and those provided by Wolfe and Upchurch [13], polar ice could have existed. The presence of ice has been proposed by Miller et al. [67] in order to account for worldwide sea-level drops during the Maastrichtian. Deep water temperature of about 5 °C, calculated from  $\delta^{18}\text{O}$  values of foraminifera from ODP site 690 (65°S), implies the presence of ice at higher latitudes [67]. However, geological evidence for the storage of ice at high latitudes during the Mesozoic is scarce and still remains highly debated (e.g., [4]). Concerning the Campanian–Maastrichtian interval, pebbly siltstones resembling diamictites were deposited in the Campanian of North Island (New Zealand). These diamictites are poorly sorted with a matrix of angular quartz and rock flour, but no pebbles appear to be striated [68]. Erratic clasts of gneisses, granites and quartzites have also been described from the Maastrichtian of Denmark [69], but they may have been deposited from driftwood or floating seaweed rather than ice.

Subfreezing mean air temperatures at high latitudes that were deduced from the vertebrate  $\delta^{18}\text{O}$  gradient support the existence of ice at the end of the Cretaceous. According to this hypothesis, the presence of polar ice, even temporary, could be responsible for the production of cold deep marine waters. Such a source of deep water was already invoked to explain the presence of phosphorite deposits resulting from upwellings [70,71], the evolution of fish tooth  $\varepsilon_{\text{Nd}}$  values [72,73] and an increase of the water column's oxygenation [74].

### 5.3. Implications for reptile tolerance to temperature

The reconstructed Late Campanian–Middle Maastrichtian thermal gradient suggests that mean air temperatures of about 10 °C prevailed at 60° of paleolatitude (Alberta), which is the observed limit for fossil crocodile and turtle occurrences, whereas dinosaur remains were found at higher latitudes. This

temperature of 10 °C obtained for the Late Campanian–Middle Maastrichtian is far from the optimal thermal living conditions of crocodylians that range between 30 and 35 °C (see [12]). Taking into account the uncertainties associated with the  $\delta^{18}\text{O}$  proxy of paleotemperatures, it is noteworthy that this low temperature of 10 °C is however not significantly different from the mean temperature of 13–14 °C tolerated by the extant alligatorid *Alligator mississippiensis* living in its natural environment. The temperature of the coldest month, too cold for a crocodylian to survive, typically ranges between 5 and 10 °C ([75,76]). According to Wolfe and Upchurch [13] and our isotopic data, the coldest month mean temperature at 60°N would be about 6 °C during the Campanian and Maastrichtian. A relatively diverse crocodylian fauna is known from the Campanian of Alberta. Our results suggest that like the recent genus *Alligator*, these crocodylians were able to tolerate relatively low winter temperatures, possibly by hibernating, as extant alligators do.

Above this key paleolatitude of 60°, the only tetrapods documented so far during the Campanian–Maastrichtian are dinosaurs, birds and mammals. The latter two were undoubtedly endothermic vertebrates that could tolerate mean air temperatures below 10 °C. The case of dinosaur thermophysiology is still unclear. Although several lines of argument [24,34,77,78] support the hypothesis that at least some of them possessed an intermediate to high metabolic level, simulations from computer models [23,25] and interpretations of preserved structures such as lung imprints [79] and nasal cavities [26] tend to be in favour of ectothermic dinosaurs. Although the debate on dinosaur thermophysiology is not yet clearly resolved, both the distribution of tetrapods and our temperature estimates at high latitudes during the Campanian–Maastrichtian suggest that at least some dinosaurs had developed thermal strategies which enabled them to live in polar areas where mean air temperatures and seasonality were unsuitable for ectothermic reptiles and amphibians.

## 6. Concluding remarks

The present-day transfer function established between vertebrate apatite  $\delta^{18}\text{O}$  values, meteoric

waters  $\delta^{18}\text{O}$  values and mean annual air temperatures was applied to  $\delta^{18}\text{O}$  values of fossil reptiles to restore a latitudinal thermal gradient for the Late Campanian–Middle Maastrichtian. The good consistency between the computed continental temperature gradient and other published temperature estimates suggests that the method developed in this study is relevant to paleoclimatic reconstructions.

The following results are underlined:

- during the Late Campanian–Middle Maastrichtian interval, the latitudinal temperature gradient was weaker (about  $0.4 \pm 0.1$  °C/°latitude) than today ( $0.6$  °C/°latitude).
- low latitude paleotemperatures were similar to present-day temperatures, whereas freezing conditions only possibly occurred above  $80^\circ$  paleolatitude.
- polar temperatures ranged between  $-10$  and  $0$  °C, assuming the relatively high equability proposed by Wolfe and Upchurch [13]. They support the existence of ice at high latitudes that could have been responsible for the production of deep marine water.
- the occurrence of fossil crocodylians up to paleolatitudes of  $60^\circ$  suggests that these ectotherms were able to live in relatively cold environments with mean air temperatures of  $10 \pm 4$  °C. It is noteworthy that similar mean air temperatures are tolerated by the extant alligatorid *Alligator mississippiensis*, and thus, our results do not imply unexpected or unusual physiological adaptations in Late Campanian–Middle Maastrichtian high-latitude crocodylians.

## Acknowledgements

The authors would like to thank the Royal Tyrell Museum (Drumheller, Canada) and the Musée de l'ACAP (Cruzy, France) for providing materials and Gilles Escarguel for his constructive comments. An early version of this manuscript benefited from comments and editorial corrections made by V. Daux, S.M.F. Sheppard and T.W. Vennemann. The authors are also grateful to L. Frakes and G. Price for their helpful reviews. This study was supported by the 'ECLIPSE'

program of the Centre National de la Recherche Scientifique.

## Appendix A. Annex 1

Numerous data for present-day oxygen isotope compositions of mammalian apatites (bones and teeth) have been published [30,31,80–92]. Meteoritic water  $\delta^{18}\text{O}$  values and sometimes relative humidity were used to calculate oxygen isotope fractionation equations between phosphate ( $\delta^{18}\text{O}_p$ ) and water ( $\delta^{18}\text{O}_w$ ) [84,88,93].

Data were compiled, excluding zoo animal values [90]. Based on the location provided for each specimen, the  $\delta^{18}\text{O}_{\text{meteoric water}}$  values were calculated using the IAEA–WMO data [18] and corrected from latitude and altitude when available. Otherwise, when location was not precise enough, we used an IAEA–WMO station from the same country for which the  $\delta^{18}\text{O}_w$  was similar to that provided in the original work. The following values for adjustment were used:  $-0.5\%$  per degree latitude and  $-0.3\%$  per 100 m of elevation [94]. Each  $\delta^{18}\text{O}_p$  is then associated with mean annual and to mean monthly minimum and maximum  $\delta^{18}\text{O}_w$ . This database is available upon request as electronic supplement.

Determination coefficient between published  $\delta^{18}\text{O}_w$  and  $\delta^{18}\text{O}_p$  is rather high ( $R^2=0.798$  with  $n=379$ ; Fig. 7A). But, using recalculated mean annual values  $\delta^{18}\text{O}_w$ ,  $R^2$  is higher ( $R^2=0.831$  with  $n=427$ ). The equation is:  $\delta^{18}\text{O}_w=1.0058 (\pm 0.0219) \times \delta^{18}\text{O}_p - 24.9315 (\pm 0.4070)$ . The  $\delta^{18}\text{O}_w$  varies over the year, and monthly values vary over several years, the range between minimum and maximum annual  $\delta^{18}\text{O}_w$  increasing with latitude. In order to maximize the relationship between both parameters,  $\delta^{18}\text{O}_w$  values were estimated on the basis of regression coefficients of the least square regression between mean annual  $\delta^{18}\text{O}_w$  and  $\delta^{18}\text{O}_p$ . If the estimated value was included in the monthly minimum–maximum interval, then it was used for calculating a maximized  $R^2$ ; otherwise, the minimum or maximum value was retained. After removing some outliers, the regression equation is:  $\delta^{18}\text{O}_w=0.9654 (\pm 0.0063) \times \delta^{18}\text{O}_p - 24.2784 (\pm 0.1166)$ , with  $R^2=0.982$ ,  $n=427$ . If marsupials are omitted (Fig. 7B), the equation becomes:  $\delta^{18}\text{O}_w=1.1128 (\pm 0.0029) \times \delta^{18}\text{O}_p - 26.4414 (\pm 0.0508)$ , with  $R^2=0.998$ ,  $n=368$ .

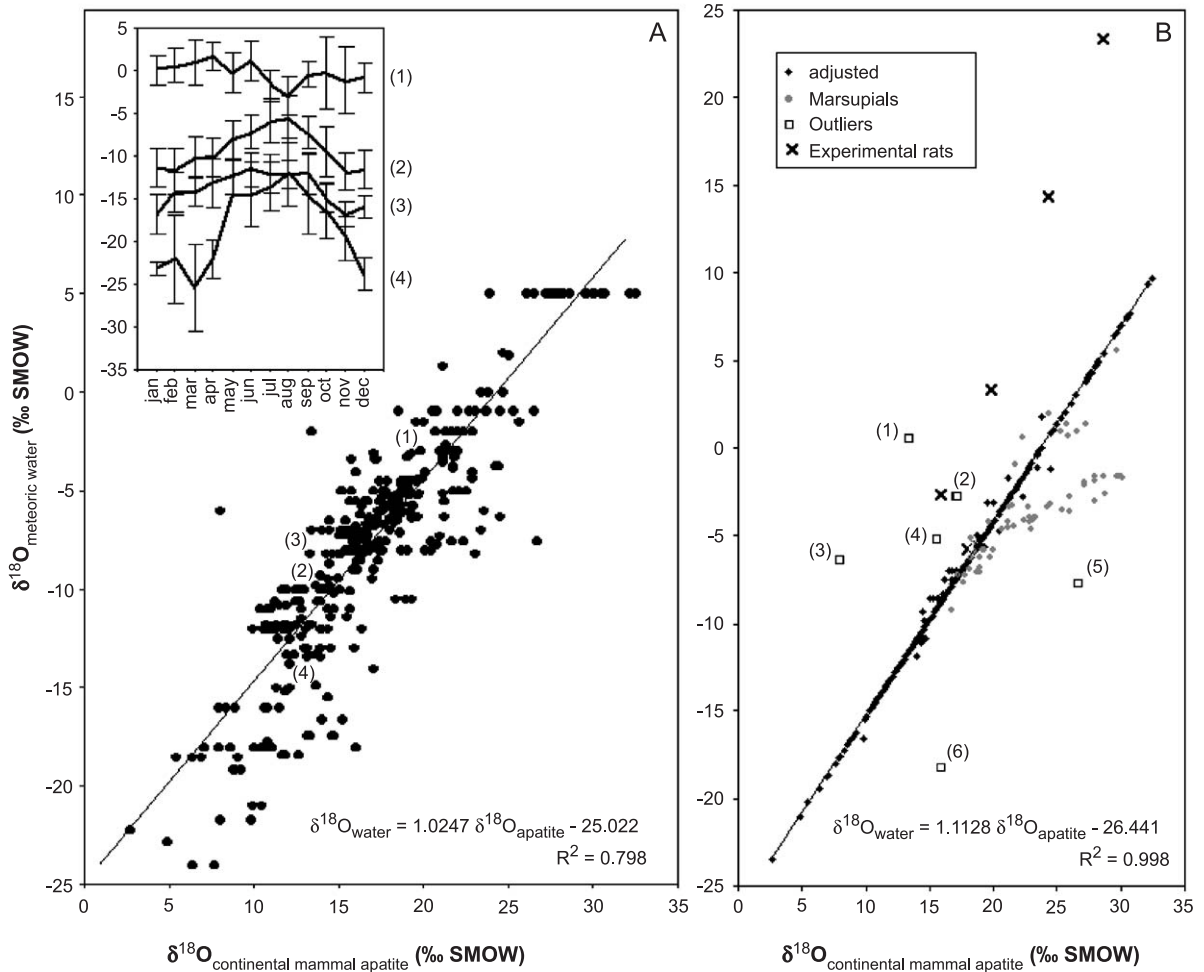


Fig. 7. Relation between  $\delta^{18}\text{O}$  values of meteoric waters and of mammalian apatites (bones and teeth) for published data (A) and adjusted  $\delta^{18}\text{O}_w$  (B). (A) Each  $\delta^{18}\text{O}_p$  has been published with one  $\delta^{18}\text{O}_w$  (see text for references). But at each location, this value varies within 1 year and over years, as shown in the upper left inset, with mean monthly values (and standard error) for the following stations:

- (1) Addis Ababa, Ethiopia;
- (2) Thonon-les-Bains, France;
- (3) Lapptrask, Iceland;
- (4) Barrow, Alaska.

(B) Published  $\delta^{18}\text{O}_p$  are fitted with values taken in the various minimum–maximum monthly  $\delta^{18}\text{O}_w$  intervals. The regression coefficient is then very high, when marsupials and outliers are omitted. The outliers are:

- (1) *Equus burchelli*, Sudan;
- (2) *Homo*, Honolulu, Hawaii;
- (3) *Homo*, Indianapolis, Indiana;
- (4) *Equus zebra*, South Africa;
- (5) *Equus caballus*, New York State;
- (6) *Canis lupus*, Arctic Circle.

## References

- [1] E.S. Barron, A warm, equable Cretaceous; the nature of the problem, *Earth Sci. Rev.* 19 (1983) 305–338.
- [2] A. Hallam, A review of Mesozoic climate, *J. Geol. Soc. (Lond.)* 142 (1985) 433–445.
- [3] L.A. Frakes, *Climates Throughout Geologic Time*, Elsevier, Amsterdam, 1979, 310 pp.
- [4] G.D. Price, The evidence and implications of polar ice during the Mesozoic, *Earth Sci. Rev.* 48 (1999) 183–210.
- [5] B. van de Schootbrugge, K.B. Foellmi, L.G. Bulot, S.J. Burns, Paleoclimatographic changes during the Early Cretaceous (Valanginian–Hauterivian): evidence from oxygen and carbon stable isotopes, *Earth Planet. Sci. Lett.* 181 (2000) 15–31.
- [6] D.R. Groecke, G.D. Price, A.H. Ruffell, J. Mutterlose, E. Baraboshkin, Isotopic evidence for Late Jurassic–Early Cretaceous climate change, *Palaeogeogr. Palaeoclimatol. Palaeoecol.* 202 (2003) 97–118.
- [7] E. Pucéat, C. Lécuyer, S.M.F. Sheppard, G. Dromart, S. Reboulet, P. Grandjean, Thermal evolution of Cretaceous Tethyan marine waters inferred from oxygen isotope composition of fish tooth enamels, *Paleoceanography* 18 (2003) 7–12.
- [8] R.A. Berner, Z. Kothavala, GEOCARB. III: a revised model of atmospheric CO<sub>2</sub> over Phanerozoic time, *Am. J. Sci.* 301 (2001) 182–204.
- [9] B.U. Haq, J. Hardenbol, P.R. Vail, Mesozoic and Cenozoic chronostratigraphy and cycles of sea-level change, *Spec. Publ.-Soc. Econ. Paleontol. Mineral.* 42 (1988) 72–108.
- [10] E.J. Barron, P.J. Fawcett, W.H. Peterson, D. Pollard, S.L. Thompson, A “simulation” of Mid-Cretaceous climate, *Paleoceanography* 10 (1995) 953–962.
- [11] W.A. Clemens, L.G. Nelms, Paleocological implications of Alaskan terrestrial vertebrate fauna in latest Cretaceous time at high paleolatitudes: reply [modified], *Geology* 21 (1993) 1152.
- [12] P.J. Markwick, Fossil crocodylians as indicators of Late Cretaceous and Cenozoic climates; implications for using palaeontological data in reconstructing palaeoclimate, *Palaeogeogr. Palaeoclimatol. Palaeoecol.* 137 (1998) 205–271.
- [13] J.A. Wolfe, G.R. Upchurch Jr., North American nonmarine climates and vegetation during the Late Cretaceous, *Palaeogeogr. Palaeoclimatol. Palaeoecol.* 61 (1987) 33–77.
- [14] J.T. Parrish, R.A. Spicer, Late Cretaceous terrestrial vegetation; a near-polar temperature curve, *Geology* 16 (1988) 22–25.
- [15] J.E. Francis, I. Poole, Cretaceous and Early Tertiary climates of Antarctica; evidence from fossil wood, in: J.E. Francis, M.P. Smith (Eds.), *Palaeogeogr. Palaeoclimatol. Palaeoecol.*, 182, Elsevier, Amsterdam, 2002, pp. 47–64.
- [16] L.A. Frakes, J.-L. Probst, W. Ludwig, Latitudinal distribution of paleotemperature on land and sea from Early Cretaceous to middle Miocene, *C. R. Acad. Sci.* 318 (1994) 1209–1218.
- [17] K. Rozanski, L. Araguas-Araguas, R. Gonfiantini, Isotopic patterns in modern global precipitation, *Geophys. Monogr.* 78 (1993) 1–36.
- [18] IAEA/WMO, Global Network of Isotopes in Precipitation. The GNIP Database. Accessible at: <http://www.isohis.iaea.org>, 2001.
- [19] M.A. Poage, C.P. Chamberlain, Empirical relationships between elevation and the stable isotope composition of precipitation and surface waters; considerations for studies of paleoelevation change, *Am. J. Sci.* 301 (2001) 1–15.
- [20] G.J. Bowen, B. Wilkinson, Spatial distribution of  $\delta^{18}\text{O}$  in meteoric precipitation, *Geology* 30 (2002) 315–318.
- [21] R.E. Barrick, A.G. Fischer, W.J. Showers, Oxygen isotopes from turtle bone: application for terrestrial paleoclimates? *Palaios* 14 (1999) 186–191.
- [22] Y. Kolodny, B. Luz, O. Navon, Oxygen isotope variations in phosphate of biogenic apatites: I. Fish bone apatite; rechecking the rules of the game, *Earth Planet. Sci. Lett.* 64 (1983) 398–404.
- [23] J.R. Spotila, M.P. O’Connor, P. Dodson, F.V. Paladino, Anonymous, Hot and cold running dinosaurs; body size, metabolism and migration, *Mod. Geol.* 16 (1991) 203–227.
- [24] R.E. Barrick, W.J. Showers, Thermophysiology of *Tyrannosaurus rex*: evidence from oxygen isotopes, *Science* 265 (1994) 222–224.
- [25] M.P. O’Connor, P. Dodson, Biophysical constraints on the thermal ecology of dinosaurs, *Paleobiology* 25 (1999) 341–368.
- [26] J.A. Ruben, W.J. Hillenius, N.R. Geist, A. Leitch, T.D. Jones, P.J. Currie, J.R. Horner, G. Espe III, The metabolic status of some Late Cretaceous dinosaurs, *Science* 273 (1996) 1204–1207.
- [27] R.E. Barrick, The thermodynamics of dinosaurs, in: G.S. Paul (Ed.), *The Scientific American Book of Dinosaurs*, St. Martin’s Press, New York, 2000, pp. 310–322.
- [28] W. Dansgaard, Stable isotopes in precipitation, *Tellus* 16 (1964) 436–468.
- [29] U. von Grafenstein, H. Erlenkeuser, J. Mueller, P. Trumborn, J. Ales, A 200 year mid-European air temperature record preserved in lake sediments; an extension of the  $\delta^{18}\text{O}_p$ -air temperature relation into the past, *Geochim. Cosmochim. Acta* 60 (1996) 4025–4036.
- [30] A. Longinelli, Oxygen isotopes in mammal bone phosphate; a new tool for paleohydrological and paleoclimatological research? *Geochim. Cosmochim. Acta* 48 (1984) 385–390.
- [31] B. Luz, Y. Kolodny, M. Horowitz, Fractionation of oxygen isotopes between mammalian bone-phosphate and environmental drinking water, *Geochim. Cosmochim. Acta* 48 (1984) 1689–1693.
- [32] Y. Yurtsever, Worldwide survey of stable isotopes in precipitation, *Rep. Sect. Isotope Hydrol.*, IAEA (1975) 40.
- [33] Y. Kolodny, B. Luz, M. Sander, W.A. Clemens, Dinosaur bones: fossils or pseudomorphs? The pitfalls of physiology reconstruction from apatitic fossils, *Palaeogeogr. Palaeoclimatol. Palaeoecol.* 126 (1996) 161–171.
- [34] H.C. Fricke, R.R. Rogers, Multiple taxon–multiple locality approach to providing oxygen isotope evidence for warm-blooded theropod dinosaurs, *Geology* 28 (2000) 799–802.
- [35] J. Besse, V. Courtillot, Paleogeographic maps of the continents bordering the Indian Ocean since the Early Jurassic, *J. Geophys. Res.* 93 (1988) 11791–11808.



- [36] J. Besse, V. Courtillot, Revised and synthetic apparent polar wander paths of the African, Eurasian, North American and Indian Plates, and true polar wander since 200 Ma, *J. Geophys. Res.* 96 (1991) 4029–4050.
- [37] J. Besse, V. Courtillot, Apparent and true polar wander and the geometry of the geomagnetic field over the last 200 Myr, *J. Geophys. Res.* 107 (2003) 2300.
- [38] Y. Chen, V. Courtillot, J.P. Cogné, J. Besse, Z. Yang, R. Enkin, The configuration of Asia prior to the collision of India: Cretaceous paleomagnetic constrains, *J. Geophys. Res.* 98 (1993) 21927–21941.
- [39] G.S. Odin, Numerical age calibration of the Campanian–Maastrichtian succession at Tercis les Bains (Landes, France) and in the Bottaccione Gorge (Italy), in: G.S. Odin (Ed.), *The Campanian–Maastrichtian stage boundary*, Elsevier, Amsterdam, 2001, pp. 775–782.
- [40] E. Buffetaut, J. Le Loeuff, H. Tong, S. Duffaud, L. Cavin, G. Garcia, D. Ward, Un nouveau gisement de vertébrés du Crétacé supérieur à Cruzy (Hérault, Sud de la France), *C. R. Acad. Sci.* 328 (1999) 203–208.
- [41] D.A. Eberth, A.P. Hamblin, Tectonic, stratigraphic, and sedimentologic significance of a regional discontinuity in the upper Judith River Group (Belly River wedge) of southern Alberta, Saskatchewan, and northern Montana, *Can. J. Earth Sci.* 30 (1993) 174–200.
- [42] M. Gayet, L.G. Marshall, T. Sempere, F.J. Meunier, H. Cappetta, J.-C. Rage, Middle Maastrichtian vertebrates (fishes, amphibians, dinosaurs and other reptiles, mammals) from Pajcha Pata (Bolivia). Biostratigraphic, palaeoecologic and palaeobiogeographic implications, *Palaeogeogr. Palaeoclimatol. Palaeoecol.* 169 (2001) 39–68.
- [43] R.A. Crowson, W.J. Showers, E.K. Wright, T.C. Hoering, A method for preparation of phosphate samples for oxygen isotope analysis, *Anal. Chem.* 63 (1991) 2397–2400.
- [44] C. Lécuyer, P. Grandjean, J.R. O’Neil, H. Cappetta, F. Martineau, Thermal excursions in the ocean at Cretaceous–Tertiary boundary (northern Morocco):  $\delta^{18}\text{O}$  record of phosphatic fish debris, *Palaeogeogr. Palaeoclimatol. Palaeoecol.* 105 (1993) 235–243.
- [45] C. Lécuyer, P. Grandjean, J.-A. Barrat, J. Nolvak, C. Emig, F. Paris, M. Robardet, delta (super 18) O and REE contents of phosphatic brachiopods; a comparison between modern and lower Paleozoic populations, *Geochim. Cosmochim. Acta* 62 (1998) 2429–2436.
- [46] J.R. O’Neil, L.J. Roe, E. Reinhard, R.E. Blake, A rapid and precise method of oxygen isotope analysis of biogenic phosphate, *Isr. J. Earth-Sci.* 43 (1994) 203–212.
- [47] R.E. Blake, J.R. O’Neil, G.A. Garcia, Oxygen isotope systematics of biologically mediated reactions of phosphate: I. Microbial degradation of organophosphorus compounds, *Geochim. Cosmochim. Acta* 61 (1997) 4411–4422.
- [48] A. Zazzo, C. Lécuyer, A. Mariotti, Experimentally-controlled carbon and oxygen isotope exchange between bioapatites and water under inorganic and microbially-mediated conditions, *Geochim. Cosmochim. Acta* 68 (2004) 1–12.
- [49] C. Lécuyer, P. Grandjean, S.M.F. Sheppard, Oxygen isotope exchange between dissolved phosphate and water at temperatures  $<135\text{ }^{\circ}\text{C}$ : inorganic versus biological fractionations, *Geochim. Cosmochim. Acta* 63 (1999) 855–862.
- [50] Y. Kolodny, M. Raab, Oxygen isotopes in phosphatic fish remains from Israel; paleothermometry of tropical Cretaceous and Tertiary shelf waters, *Palaeogeogr. Palaeoclimatol. Palaeoecol.* 64 (1988) 59–67.
- [51] C. Lécuyer, C. Bogy, J.P. Garcia, P. Grandjean, J.A. Barrat, M. Floquet, N. Bardet, X. Pereda-Superbiola, Stable isotope composition and rare earth element content of vertebrate remains from the Late Cretaceous of northern Spain (Lano); did the environmental record survive? *Palaeogeogr. Palaeoclimatol. Palaeoecol.* 193 (2003) 457–471.
- [52] S. Picard, J.-P. Garcia, C. Lécuyer, S.M.F. Sheppard, H. Cappetta, C.C. Emig,  $\delta^{18}\text{O}$  values of coexisting brachiopods and fish; temperature differences and estimates of paleo-water depths, *Geology* 26 (1998) 975–978.
- [53] H.C. Fricke, W.C. Clyde, J.R. O’Neil, P.D. Gingerich, Evidence for rapid climate change in North America during the latest Paleocene thermal maximum; oxygen isotope compositions of biogenic phosphate from the Bighorn Basin (Wyoming), *Earth Planet. Sci. Lett.* 160 (1998) 193–208.
- [54] W.H. Straight, R.E. Barrick, D.A. Eberth, Reflections of surface water, seasonality and climate in stable oxygen isotopes from tyrannosaurid tooth enamel, *Palaeogeogr. Palaeoclimatol. Palaeoecol.* 206 (2004) 239–256.
- [55] E.M. Kennedy, R.A. Spicer, P.M. Rees, Quantitative palaeoclimate estimates from Late Cretaceous and Paleocene leaf floras in the northwest of the South Island, New Zealand, *Palaeogeogr. Palaeoclimatol. Palaeoecol.* 184 (2002) 321–345.
- [56] E. Barrera, B.T. Huber, S.M. Savin, P.-N. Webb, Antarctic marine temperatures; late Campanian through early Paleocene, *Paleoceanography* 2 (1987) 21–47.
- [57] S. D’Hondt, M.A. Arthur, Late Cretaceous oceans and the cool tropic paradox, *Science* 271 (1996) 1838–1841.
- [58] P.W. Ditchfield, J.D. Marshall, D. Pirrie, High latitude palaeotemperature variation; new data from the Tithonian to Eocene of James Ross Island, Antarctica, *Palaeogeogr. Palaeoclimatol. Palaeoecol.* 107 (1994) 79–102.
- [59] L.A. Frakes, Estimating the global thermal state from Cretaceous sea surface and continental temperature data, *Spec. Pap.-Geol. Soc. Am.* 332 (1999) 49–57.
- [60] E.J. Barron, W.M. Washington, Warm Cretaceous climates, high atmospheric  $\text{CO}_2$  as a plausible mechanism, *Geophys. Monogr.* 32 (1985) 546–553.
- [61] C. Covey, E.J. Barron, The role of ocean heat transport in climatic change, *Earth Sci. Rev.* 24 (1988) 429–445.
- [62] G.A. Schmidt, L.A. Mysak, Can increased poleward oceanic heat flux explain the warm Cretaceous climate? *Paleoceanography* 11 (1996) 579–593.
- [63] E.C. Brady, R.M. DeConto, S.L. Thompson, Deep water formation and poleward heat transport in the warm climate extreme of the Cretaceous (80 Ma), *Geophys. Res. Lett.* 25 (1998) 4205–4208.
- [64] R.M. DeConto, E.C. Brady, J. Bergengren, W.W. Hay, Late Cretaceous climate, vegetation, and ocean interactions, in: B.T. Huber, K.G. MacLeod, S.L. Wing (Eds.), *Warm Climates in*

- Earth History, Cambridge University Press, Cambridge, 2000, pp. 275–296.
- [65] C. Lécuyer, P. Grandjean, J.-M. Mazin, V. De Buffrénil, Oxygen isotope compositions of reptile bones and teeth: a potential record of terrestrial and marine paleoenvironments, in: E. Hoch, A.K. Brantsen (Eds.), *Secondary Adaptation to Life in Water II*, University of Copenhagen (Denmark), Geologisk Museum, 1999, p. 33.
- [66] J.A. Wolfe, A method of obtaining climate parameters from leaf assemblages, *U.S. Geol. Surv. Bull.* 2040 (1993) (71 pp.).
- [67] K.G. Miller, E. Barrera, R.K. Olsson, P.J. Sugarman, S.M. Savin, Does ice drive early Maastrichtian eustasy? *Geology* 27 (1999) 783–786.
- [68] J.B. Waterhouse, P.G. Flood, M.J. Hambrey, W.B. Harland, Poorly Sorted Conglomerates, Breccias and Diamictites in Late Palaeozoic, Mesozoic and Tertiary Sediments of New Zealand, Cambridge Univ. Press, Cambridge, 1981.
- [69] A. Noe-Nygaard, Erratics of the Danish Maastrichtian and Danian marine limestones, *Bull. Geol. Soc. Den.* 24 (1975) 75–81.
- [70] P.J. Cook, J.R. Cook, J. Lucas, L. Prevot, Marine biological changes and phosphogenesis around the Cretaceous–Tertiary boundary, *Sci. Géol. Mém.* 77 (1985) 105–108.
- [71] J. Lucas, L. Prevot-Lucas, Tethyan phosphates and bioproducts, in: A.E.M. Nairn, L.-E. Ricou, B. Vrielynck, J. Dercourt (Eds.), *The Ocean Basins and Margins: The Tethyan Ocean* 8, Plenum Press, New York, 1995, pp. 367–391.
- [72] P. Grandjean, H. Cappetta, A. Michard, F. Albarede, The assessment of REE patterns and  $^{143}\text{Nd}/^{144}\text{Nd}$  ratios in fish remains, *Earth Planet. Sci. Lett.* 84 (1987) 181–196.
- [73] P. Stille, M. Steinmann, S.R. Riggs, Nd isotope evidence for the evolution of the paleocurrents in the Atlantic and Tethys oceans during the past 180 Ma, *Earth Planet. Sci. Lett.* 144 (1996) 9–19.
- [74] C. Lécuyer, B. Reynard, P. Grandjean, Rare earth element evolution of Phanerozoic seawater recorded in biogenic apatites, *Chem. Geol.* 204 (2004) 63–102.
- [75] E.H. Colbert, R.B. Cowles, C.M. Bogert, Temperature tolerances in the American alligator and their bearing on the habits, evolution and extinction of the dinosaurs, *Bull. Am. Mus. Nat. Hist.* 86 (1946) 327–374.
- [76] D.E. Berg, Krokodile als Klimazeugen, *Geol. Rundsch.* 54 (1964) 328–333.
- [77] R.E. Barrick, W.J. Showers, Oxygen isotope variability in juvenile dinosaurs (*Hypacrosaurus*): evidence for thermoregulation, *Paleobiology* 21 (1995) 552–560.
- [78] R.E. Barrick, W.J. Showers, A.G. Fischer, Comparison of thermoregulation of four Ornithischian dinosaurs and a Varanid lizard from the Cretaceous Two Medicine formation: evidence from oxygen isotopes, *Palaos* 11 (1996) 295–305.
- [79] J.A. Ruben, C. Dal Sasso, N.R. Geist, W.J. Hillenius, T.D. Jones, M. Signore, Pulmonary function and metabolic physiology of theropod dinosaurs, *Science* 283 (1999) 514–516.
- [80] B. Luz, Y. Kolodny, J. Kovach, Oxygen isotope variations in phosphate of biogenic apatites: III. Conodonts, *Earth Planet. Sci. Lett.* 69 (1984) 255–262.
- [81] B. Luz, Y. Kolodny, Oxygen isotope variations in phosphate of biogenic apatites: IV. Mammal teeth and bones, *Earth Planet. Sci. Lett.* 75 (1985) 26–29.
- [82] A.A. Levinson, B. Luz, Y. Kolodny, Variations in oxygen isotopic compositions of human teeth and urinary stones, *Appl. Geochem.* 2 (1987) 367–371.
- [83] L.K. Ayliffe, A.R. Chivas, Bone phosphate oxygen-isotopes of modern elephants. Research School of Earth Science, Annual Report, 1989.
- [84] L.K. Ayliffe, A.R. Chivas, Oxygen isotope composition of the bone phosphate of Australian kangaroos-potential as a palaeoenvironmental recorder, *Geochim. Cosmochim. Acta* 54 (1990) 2603–2609.
- [85] D. D’Angela, A. Longinelli, Oxygen isotopes in living mammal’s bone phosphate: further results, *Chem. Geol.* 86 (1990) 75–82.
- [86] J.D. Bryant, B. Luz, P.N. Froelich, Oxygen isotopic composition of fossil horse tooth phosphate as a record of continental paleoclimate, *Palaeogeogr. Palaeoclimatol. Palaeoecol.* 107 (1994) 303–316.
- [87] B. Sanchez Chillon, M. Alberdi, G. Leone, F.P. Bonadonna, B. Stenni, A. Longinelli, Oxygen isotopic composition of fossil equid tooth and bone phosphate: an archive of difficult interpretation, *Palaeogeogr. Palaeoclimatol. Palaeoecol.* 107 (1994) 317–328.
- [88] A. Delgado Huertas, P. Iacumin, B. Stenni, B. Sanchez Chillon, A. Longinelli, Oxygen isotope variations of phosphate in mammalian bone and tooth enamel, *Geochim. Cosmochim. Acta* 59 (1995) 4299–4305.
- [89] M.J. Kohn, M.J. Schoeninger, J.W. Valley, Herbivore tooth oxygen isotope compositions; effects of diet and physiology, *Geochim. Cosmochim. Acta* 60 (1996) 3889–3896.
- [90] E. Reinhard, T. de Torres, J.R. O’Neil,  $^{18}\text{O}/^{16}\text{O}$  ratios of cave bear tooth enamel: a record of climate variability during the Pleistocene, *Palaeogeogr. Palaeoclimatol. Palaeoecol.* 126 (1996) 45–49.
- [91] H.L.Q. Stuart-Williams, H.P. Schwarcz, Oxygen isotopic determination of climatic variation using phosphate from beaver bone, tooth enamel, and dentine, *Geochim. Cosmochim. Acta* 61 (1997) 2539–2550.
- [92] P. Iacumin, A. Longinelli, Relationship between  $\delta^{18}\text{O}$  values for skeletal apatite from reindeer and foxes and yearly mean  $\delta^{18}\text{O}$  values of environmental water, *Earth Planet. Sci. Lett.* 201 (2002) 213–219.
- [93] B. Luz, A.B. Cormie, H.P. Schwarcz, Oxygen isotope variations in phosphate of deer bones, *Geochim. Cosmochim. Acta* 54 (1990) 1723–1728.
- [94] U. Siegenthaler, H. Oeschger, Correlation of  $\delta^{18}\text{O}$  in precipitation with temperature and altitude, *Nature* 285 (1980) 314–317.
- [95] O. Hammer, D.A.T. Harper, P.D. Ryan, PAST–PALaeontological STatistics ver. 1.21. Available at. <http://www.folk.uio.no/ohammer/past>, 2004.